Results in Engineering 15 (2022) 100502

Contents lists available at ScienceDirect

Results in Engineering

journal homepage: www.sciencedirect.com/journal/results-in-engineering

Bio-additives from glycerol acetylation with acetic acid: Chemical equilibrium model

Federico M. Perez [a,b], Martín N. Gatti [a,b], Nora N. Nichio [a,b], Francisco Pompeo [a,b,*]

[a] CINDECA, Facultad de Ciencias Exactas, Universidad Nacional de La Plata. CCT La Plata- CONICET, 47 N.° 257, 1900, La Plata, Argentina
[b] Facultad de Ingeniería, Universidad Nacional de La Plata, 1 Esq. 47, 1900, La Plata, Argentina

ARTICLE INFO

Keywords:
Biomass
Glycerol
Acetic acid
Esterification
Chemical equilibrium
Gibbs free energy minimization

ABSTRACT

In this work, the chemical equilibrium of glycerol (G) acetylation with acetic acid (AA) to form mono- (MAG), di- (DAG) and tri- (TAG) acetylglycerols has been studied. These compounds are biodegradable and renewable options as high-quality bio-additives to improve the antiknock properties and the viscosity of fuels and biofuels.

Due to the absence of thermodynamic data, the physicochemical and thermodynamic properties of the compounds were determined, such as the specific heat, and the enthalpy and entropy of formation, by employing a second-order group-additivity predictive method. The values obtained were validated with few experimental data available in the literature (298 K, 101.325 kPa), showing differences in the range 0.2–8.9%.

The compositions at equilibrium were calculated by minimizing the total Gibbs free energy of the system and considering the non-ideality of the liquid phase. For this purpose, different temperatures (350–500 K), reactant molar ratios (1–12) and initial water contents (0 and 40 wt%) were studied. The results revealed the global exothermicity of the system, showing that total glycerol conversion (~100%) and high yields to TAG (>90%) can be achieved in the 350–500 K range by employing AA:G molar ratios between 9 and 12. As the presence of water in the glycerol solution produces a decrease of the glycerol conversion and selectivity to TAG, its removal from the reaction medium should be considered. A comparison between our results with the reported data based on different catalytic systems indicates that this model could successfully describe the chemical equilibrium of the system.

Credit author statement

Federico M. Perez Methodology, Formal analysis, Investigation, Data curation, Writing original draft. Martín N. Gatti: Investigation, Formal analysis, Writing - Review & Editing. Nora N. Nichio: Conceptualization, Funding adquisition, Resources. Francisco Pompeo: Conceptualization, Methodology, Supervision, Validation, Project administration, Writing-Reviewing and Editing.

1. Introduction

Nowadays, the need to reduce the dependence on fossil fuels has led scientists to center their research on sustainable, economic chemical processes. In this context, biomass-derived products based on organic polyfunctional molecules have been employed to substitute fine products traditionally synthetized by the petrochemical industry. Glycerol obtained as a byproduct during the synthesis of biodiesel [1], has been particularly considered as a useful platform molecule, due to its reactivity in different reactions, such as reforming [2], acetalization [3], hydrogenolysis [4], and so on, to produce valuable chemical products.

One of the promising methods to convert glycerol into high-value chemicals is the production of acetylglycerols from glycerol (G) acetylation with acetic acid (AA) or acetic anhydride (AAN). Since AAN is more expensive and harder to be handled in practice than AA, the latter is considered more suitable in terms of environmental and cost features [5].

Glycerol acetylation with acetic acid involves consecutive steps of reversible reactions, leading to the formation of monoacetyl glycerol (1-MAG and 2-MAG), diacetyl glycerol (1,2-DAG and 1,3-DAG) and triacetyl glycerol (TAG), employed in cosmetic, food and construction industries, as well as in the synthesis of biodegradable polymers (Scheme 1) [6,7]. In particular, 1,2-DAG, 1,3-DAG and TAG have been reported as high-quality bio-additives, which allow improving the antiknock properties of gasoline and the viscosity of biofuels, thus

* Corresponding author. CINDECA, Facultad de Ciencias Exactas, Universidad Nacional de La Plata. CCT La Plata- CONICET, 47 N.° 257, 1900, La Plata, Argentina.
E-mail address: fpompeo@quimica.unlp.edu.ar (F. Pompeo).

https://doi.org/10.1016/j.rineng.2022.100502
Received 20 April 2022; Received in revised form 3 June 2022; Accepted 14 June 2022
Available online 24 June 2022

enabling the replacement of methyl *tert*-butyl ether (MTBE) and ethyl *tert*-butyl ether (ETBE), which are obtained by the petrochemical route [8,9]. In this sense, the products of glycerol acetylation are a biodegradable and renewable option, being less toxic than MTBE and ETBE [10].

Glycerol acetylation with acetic acid is catalyzed by acids, in homogeneous and heterogeneous phase. In the former, organic and inorganic acids have been employed, such as p-toluene sulphonic acid [11] and H_2SO_4 [12,13], respectively, catalyzing the reaction by the Fischer esterification [14]. The employment of these acids, which are toxic and corrosive, has several drawbacks related to the design and operation [15,16]. On the one hand, reactor design requires accurate materials in order to resist corrosion. On the other hand, post-reaction treatments are needed, involving the neutralization with alkali, the elimination of the salt formed and the separation of the products of interest from the liquid effluent [17].

To overcome these limitations, acid solids with Brønsted acidity have been employed, which follow a mechanism similar to that of homogeneous catalysts, involving a first step in which the acid is adsorbed onto the solid, followed by the attack of the OH- group to the carboxylic group [18,19]. Several solids have been reported, such as cation exchange resins [20], supported heteropolyacids [21], functionalized mesoporous materials [22] and other acid solids [23,24].

Most of these reported catalysts have demonstrated high glycerol conversions (60–90%) with low selectivity to the desired products (1,2-DAG, 1,3-DAG and TAG), depending on the catalyst nature and concentration. Activity results employing these catalytic systems have revealed that both glycerol conversion and selectivity depend on the reaction conditions, such as temperature, reactants molar ratio (AA:G), water initial content and time of reaction [25]. These conditions must be optimized in order to maximize the desired products yield, but most publications are focused on the characterization of the catalyst and its relationship with the kinetic aspects of the reaction. From the point of view of the reaction, the species involved (G, AA, W, 1-MAG, 2-MAG, 1, 2-DAG, 1,3-DAG, TAG) represent a complex system, whose chemical equilibrium can be determined by employing the Gibbs free energy minimization method, which allows determining the equilibrium compositions of all species of the system, using Lagrange multipliers to incorporate the element conservation constraints [26].

Due to the absence of thermodynamic data in handbooks or databases for some of the chemical species in liquid phase (1-MAG, 2-MAG, 1,2-DAG, 1,3-DAG), predictive methods should be employed to determine enthalpy, entropy and free energy of formation, based on the chemical groups that conform the molecules.

The objective of this work is to study the chemical equilibrium of glycerol acetylation with acetic acid to form acetylglycerols. For this purpose, knowledge of thermodynamic properties is required, but they are not yet available in the literature. Because of that, the specific heat as a function of the temperature and the enthalpy and entropy of formation of all compounds involved in the reaction were calculated by employing predictive methods. With this information, the expressions of enthalpy, free Gibbs energy and entropy of reaction as a function of the temperature were obtained. The glycerol conversion at equilibrium was calculated at different temperatures by varying the initial AA:G molar ratio and water initial content, considering the non-ideality of the liquid phase. The thermodynamic and physicochemical information calculated in this contribution is essential because it is not available in simulation software. To the best of our knowledge, this is the first theoretical study on the chemical equilibrium of acetylglycerols synthesis.

2. Methodology

2.1. Definition of chemical species

In this method, chemical reactions are not specified in the traditional sense of stoichiometric equation, but present substances and their initial contents, pressure and temperature are defined. Then, the final composition was determined by employing the minimization of the total Gibbs free energy of the system, considering the mass balance of the elements. The following chemical species were considered for the thermodynamic calculus: glycerol (G), acetic acid (AA), water (W), 1-monoacetyl glycerol (1-MAG), 2-monoacetyl glycerol (2-MAG), 1,2-diacetyl glycerol (1,2-DAG), 1,3-diacetyl glycerol (1,3-DAG) and triacetyl glycerol (TAG).

2.2. Determination of the thermodynamic properties at the pressure and temperature of the system

In order to carry out the thermodynamic calculus, it is necessary to select a model for the standard chemical potential of each species, and here we use the standard molar Gibbs energy of formation. The calculation of this property involved determining the enthalpy and entropy of formation at standard conditions ($T^s = 298.15$ K, $P^s = 101.325$ kPa) and their correction with the specific heat expressions so as to obtain their values at the system conditions. The molar enthalpy of formation ($\Delta h^s_{f,i}$) and the molar entropy of formation ($\Delta s^s_{f,i}$) of each compound at standard conditions were determined by employing Equations (1) and (2), respectively, using the group contribution method developed by Domalski and Hearing, which is the most accurate and generally applicable procedure for liquids [27].

In order to determine $\Delta h^s_{f,i}$ (Eq. (1)), it was considered that each compound i was constituted by ν_j chemical groups (j = 1 … J) with molar enthalpy of formation $\Delta h^s_{f,j}$. In order to determine $\Delta s^s_{f,i}$ (Eq. (2)), it was considered that each compound i was constituted by ν_j chemical groups (j = 1 … J) with absolute molar entropy $s^s_{f,j}$, to which it was necessary to subtract the absolute molar entropy of the constituting

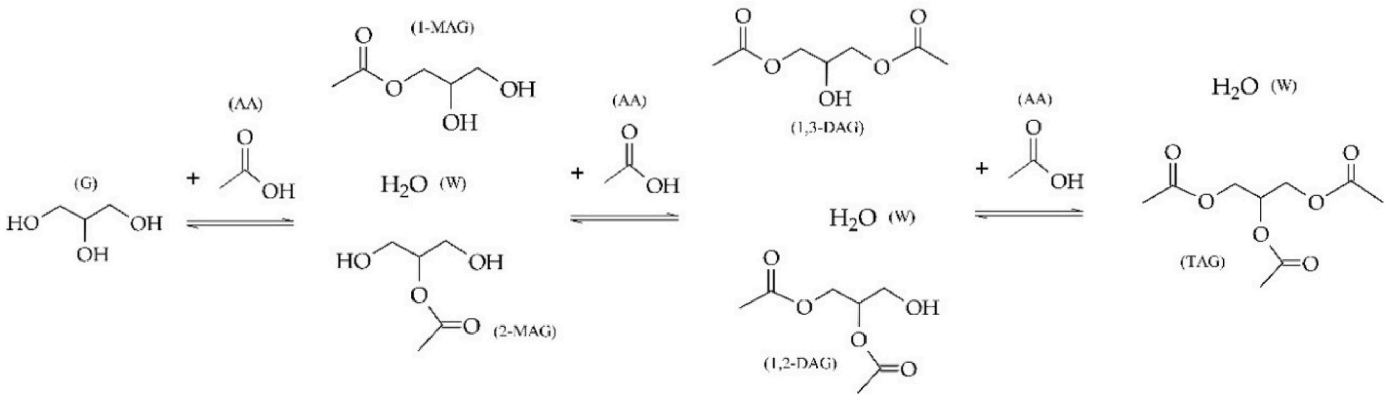

Scheme 1. Reactions involved in the glycerol acetylation with acetic acid.

elements of the compound. In this sense, s^s_m stands for the absolute molar entropy of element m, and coefficient α_m stands for the number of atoms of element m (C, H_2 and O_2) present in the compound i (m = 1 … 3). The values of $\Delta h^s_{f,j}$, $s^s_{f,j}$, $\Delta h^s_{f,i}$ and $s^s_{f,i}$ are presented in the Supplementary Information (Table S1).

$$\Delta h^s_{f,i} = \sum_{j=1}^{J} \nu_j \Delta h^s_{f,j} \tag{1}$$

$$\Delta s^s_{f,i} = \sum_{j=1}^{J} \nu_j \, s^s_{f,j} - \sum_{m=1}^{3} \alpha_m s^s_m \tag{2}$$

In order to calculate the enthalpy and entropy of formation at the system conditions, specific heat expressions of the chemical species were determined as a function of temperature ($c^0_{p,i}$ (T)). In this work, the group contribution method developed by Růžička and Domalski was employed [28], which allowed calculating the specific heat of the compounds in liquid phase, considering the interaction between an atom and its neighbor in a molecule. The specific heat expressions were determined by employing Eq. (3).

$$c^0_{p,i}(T) = R\left[B + D\frac{T}{100} + E\left(\frac{T}{100}\right)^2\right] \tag{3}$$

$$B = \sum_{j=1}^{J} \nu_j b_j \tag{3a}$$

$$D = \sum_{j=1}^{J} \nu_j d_j \tag{3b}$$

$$E = \sum_{j=1}^{J} \nu_j e_j \tag{3c}$$

Parameters b_j, d_j and e_j were obtained from the handbook of Poling-Prausnitz-O'Connell [29] and are presented in the Supplementary Information (Table S2). For water, the specific heat expression was obtained from the literature [65].

The specific heat change was expressed for each compound ($\Delta c^0_{p,i}$(T)) with respect to the specific heat of the elements (C, H_2 and O_2) that constitute them ($c^0_{p,m}$(T)), considering the stoichiometric coefficients α_m, which indicate the number of C atoms and H_2 and O_2 molecules present in each compound (Eq. (4)). The specific heat of C, H_2 and O_2 were obtained from the National Institute of Standards and Technology (NIST) [30] and are reported in the Supplementary Information (Table S3).

$$\Delta c^0_{p,i}(T) = c^0_{p,i}(T) - \sum_{m=1}^{3} \alpha_m c^0_{p,m}(T) \tag{4}$$

In order to obtain the molar Gibbs free energy of formation at the system conditions (operative P and T), the values of $\Delta h^s_{f,i}$ and $\Delta s^s_{f,i}$ calculated at standard conditions were corrected by employing Eqs. (5) and (6).

$$\Delta h^0_{f,i} = \Delta h^s_{f,i} + \int_{T^s}^{T} \Delta c^0_{p,i}(T)\, dT \tag{5}$$

$$\Delta s^0_{f,i} = \Delta s^s_{f,i} + \int_{T^s}^{T} \frac{\Delta c^0_{p,i}(T)}{T} dT \tag{6}$$

Finally, the molar Gibbs free energy of formation at the system conditions of each compound i ($\Delta g^0_{f,i}$) was calculated using Eq. (7).

$$\Delta g^0_{f,i} = \Delta h^0_{f,i} - T\Delta s^0_{f,i} \tag{7}$$

2.3. Mathematical model: thermodynamic calculus for the chemical equilibrium

For a system at constant temperature and pressure, the equilibrium state can be calculated by minimizing the free Gibbs energy with respect to the number of moles of each compound. In this work, the equilibrium calculus was solved as an optimization problem, employing the Lagrange method of undetermined multipliers with suitable constraints, such as the non-negativity of the number of moles and mass balance.

The minimization problem must satisfy the following conditions:

i Mass conservation, given by the elemental mass balance (Eq. (8)):

$$\sum_{i=1}^{N} n_i \, a_{ik} - A_k = 0 \tag{8}$$

In Eq. (8), A_k stands for the number of moles of element k (defined by the initial moles of the compounds), n_i stands for the number of moles of compound i at equilibrium, and a_{ik} stands for the number of atoms of atoms of element k present in compound i. Also, N stands for the number of compounds in the system.

ii Non-negativity of the number of moles (Eq. (9)):

$$n_i \geq 0, \quad i = 1 \ldots N \tag{9}$$

The temperature and pressure ranges studied in this work were selected to ensure that all species were in the liquid phase (T = 350–500 K and P = 2 MPa). For this reason, the phase equilibrium was omitted, and only the chemical equilibrium was considered.

Eq. (10) is obtained by defining the standard state of the compounds as pure liquids at the temperature of system (T) and a pressure of 1 atm (P^0) and expressing the partial fugacity of compound i ($\tilde{f}_i$) as a function of the activity coefficient (γ_i) and the molar fraction of compound i (x_i). Table S4 in the Supplementary Information lists the groups and group parameters of the UNIFAC method employed in the determination of the activity coefficients [64].

$$\Delta g^0_{f,i} + RTln\left(\frac{\gamma_i(x_i,T)\, x_i f^L_i(P,T)}{f^L_i(P^0,T)}\right) + \sum_{k=1}^{K} \lambda_k a_{ik} = 0 \tag{10}$$

Eq. (10) represents N equations at equilibrium (one per each compound i), and Eq. (8) represents K equations (one per each element k). If the sum of molar fractions is added, a total of N + K+1 equations are obtained. The unknown variables of the system are the N molar fractions, the K Lagrange multipliers (λ_k) and the total amount of moles (n), being a total of N + K+1 unknown variables. The system of equations was solved by applying the nonlinear conjugate gradient algorithm in Mathcad 14 Professional Software.

As the reactions occur in liquid phase, it can be assumed that the specific volumes of each compound (v^L_i) do not strongly depend on the pressure studied in this work, thus the fugacity coefficient (F_i) of Eq. (10) can be expressed as Eq. (11).

$$F_i = \frac{f^L_i(P,T)}{f^L_i(P^0,T)} = exp\left(\int_{P^0}^{P} \frac{v^L_i}{RT} dP\right) \cong exp\left[\frac{v^L_i}{RT}\left(P - P^0\right)\right] \tag{11}$$

The Yamada and Gunn correlation (Eq. (12)) was employed to calculate the saturated molar liquid volume of the compounds (v^L_i), according to Poling-Prausnitz-O'Connell recommendations [29,31].

$$v^L_i = v_{ci}\,(0.29056 - 0.08775\,\omega_i)^{\left(1-\frac{T}{T_{ci}}\right)^{2/7}} \tag{12}$$

The critical properties (T_{ci}, P_{ci}, v_{ci}) were calculated according to the Joback method [32] employing the group contribution values (t_{cj}, p_{cj} and v_{cj}) presented in the Supplementary Information (Table S5). The

normal boiling point was calculated according to Nannoolal method [33] employing the corrections for intramolecular group-group interactions reported in the Supplementary Information (Table S6). The acentric factor (ω) was calculated using the Ambrose and Walton expressions [34]. Results of physicochemical properties, normal boiling point and acentric factor of reagents and products are presented in the Supplementary Information (Table S7).

Once the compositions at equilibrium and the number of moles were determined, glycerol conversion (X_G) was calculated employing Eq. (13), where n_G^0 are the initial moles of glycerol and n_G are the moles of glycerol at equilibrium.

$$X_G(\%) = \frac{(n_G^0 - n_G)}{n_G}.100 \tag{13}$$

The selectivity towards the different products (S_i) was calculated using Eq. (14), without considering the water formed during the reaction, where n_i stands for the moles of product i calculated at equilibrium and n_{H2O} are the moles of water at equilibrium.

$$S_i(\%) = \frac{n_i}{\sum_{i=1}^{N} n_i - n_{H2O}}.100 \tag{14}$$

3. Results and discussion

3.1. Physicochemical and thermodynamic properties

Fig. 1 shows the specific heat variation of each compound ($cp_i^0(T)$) as a function of temperature. Water is not shown here as it was obtained from the literature.

In Fig. 1, a slight dependence of the specific heat of the compounds on the temperature can be observed. It has been reported that the specific heat of liquids does not strongly depend on temperature, except at reduced temperatures (T_r) above 0.8 [35]. In this work, $0.3 < T_r < 0.7$, which would explain the results obtained.

It can also be observed that the specific heat variation for glycerol is slightly higher than that of the reaction products. Phillips and Mattarnal demonstrated that the addition of carboxylic groups to a saturated hydrocarbon chain of a compound reduces the specific heat proportionally to the number of added groups [36]. The results of Fig. 1 indicate that the variation of the specific heat with temperature decreases as an –OH group of glycerol is substituted by an acetyl group (-$COCH_3$), until becoming practically linear and constant. For example, for TAG, R^2 = 0.9961. Similar results have been reported by Zhu et al. who employed modulated differential scanning calorimetry to determine the specific heat of saturated liquid triacetylglycerol and determined that it varies linearly with temperature [37].

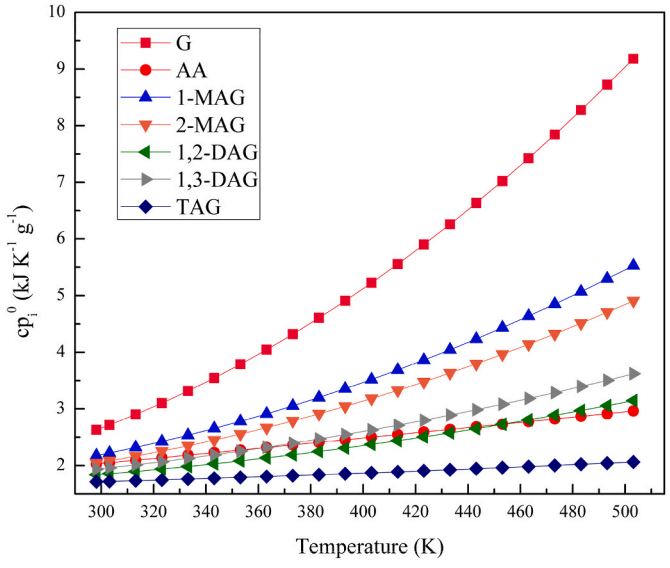

Fig. 1. Specific heat as a function of temperature for each compound involved in the reaction.

After determining the specific heat expressions for the compounds, their thermodynamic properties of formation were calculated (Fig. 2). Fig. 2a and b presents the values obtained for molar enthalpy of formation $\left(\Delta h^0_{f,i}(T)\right)$ and molar entropy of formation $\left(\Delta s^0_{f,i}(T)\right)$ as a function of the temperature. As observed, molar enthalpy and entropy of formation show a slight variation with temperature, a fact that is expected as the specific heat does not vary too much with temperature. As a consequence of that, it can be seen that the Gibbs free energy of formation varies linearly with the temperature, which is in agreement with $\Delta G = \Delta H - T\Delta S$, the terms ΔH and ΔS being almost constant. Tables S8, S9 and S10 contain the data corresponding to Fig. 2a, b and 2c, respectively.

In order to evaluate the reliability of the procedure employed in this work, the calculated values for the physicochemical and thermodynamic properties were compared with the data available in the literature, which are summarized in Table 1. Unfortunately, there is very little information about the properties of most acetylglycerols (1-MAG, 2-MAG, 1,2-DAG, 1,3-DAG), which allows comparing only the calculated values with the available data in the literature at standard conditions. Thus, the values calculated in this work may be useful for future work on this matter. As it can be observed, from Table 1, the agreement is remarkably good.

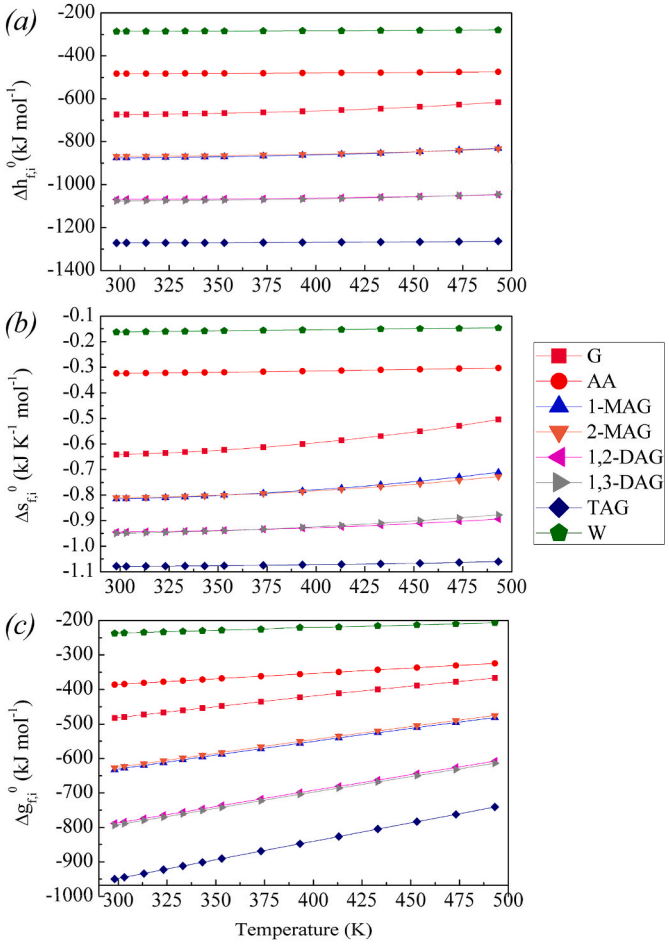

Fig. 2. Thermodynamic properties as a function of temperature for all the compounds involved in the reaction system: (a) molar enthalpy of formation ($\Delta h^0_{f,i}$) (b) molar entropy of formation ($\Delta s^0_{f,i}$) (c) molar free energy of formation ($\Delta g^0_{f,i}$).

Table 1
Comparison of the results obtained in this work with those reported in the literature. (*) NIST database; n.a: non available.

Compound	Predicted value (298.15 K)			Reported value (298.15 K) *			Difference (%)		
	cp^0 (J K^{-1} mol^{-1})	Δh_f^0 (kJ mol^{-1})	Δs_f^0 (kJ K^{-1} mol^{-1})	cp^0 (J K^{-1} mol^{-1})	Δh_f^0 (kJ mol^{-1})	Δs_f^0 (kJ K^{-1} mol^{-1})	cp^0	Δh_f^0	Δs_f^0
G	241.97	−673.7	−0.641	221.90	−669.6	−0.641	8.3	0.6	0.0
AA	121.60	−482.6	−0.324	123.10	−483.5	−0.319	1.2	0.2	1.6
1-MAG	291.36	−875.2	−0.815	n. a.	−903.5	n. a.	–	3.2	–
2-MAG	273.92	−868.6	−0.811	n. a.	n. a.	n. a.	–	–	–
1,2-DAG	323.54	−1070	−0.945	n. a.	−1121	n. a.	–	4.5	–
1,3-DAG	340.98	−1077	−0.949	n. a.	n. a.	n. a.	–	–	–
TAG	373.16	−1272	−1.088	384.70	−1331	−1.124	3.1	4.4	3.2

3.2. Acetylation reaction - Chemical equilibrium

The thermodynamic analysis of the chemical equilibrium was carried out in a temperature range of 350–500 K and AA:G molar ratios between 1 and 12. The pressure employed was 2 MPa, in order to make sure that all the compounds were in liquid phase. In these conditions, and for the specific volumes for each compound, coefficient $\frac{f_i^L(P,T)}{f_i^L(P^0,T)}$ was calculated. The results, shown in the Supplementary Information (Figure S1), indicate that this coefficient value is close to unity for all the compounds in the temperature range studied.

The acetylation reaction proceeds through the activation (protonation) of the carbonyl group of the acetic acid molecule, which is possible thanks to a strong acid catalyst (Brønsted acid generally). Then, the carbon atom of the activated carbonyl group is attacked by an –OH group of glycerol (nucleophilic attack), forming a C–O bond between the carbon atom of the carbonyl group and the oxygen atom of the –OH group. After that, this intermediate loses a water molecule to form monoacetyl glycerol (1-MAG and 2-MAG). The following reaction of MAGs with an AA molecule leads to the formation of diacetyl glycerol (1,2-DAG and 1,3-DAG), and finally TAG [38,39]. Tonutti et al. reported that, from the perspective of G, MAG, DAG and TAG, it is a serial mechanism, and, from the perspective of AA and W, it consists of three parallel reactions [40]. A possible reaction mechanism is presented in Eqs. (15)–(21).

$$G + AA \leftrightarrow 1\text{-MAG} + W \quad (15)$$

$$G + AA \leftrightarrow 2\text{-MAG} + W \quad (16)$$

$$1\text{-MAG} + AA \leftrightarrow 1,3\text{-DAG} + W \quad (17)$$

$$1\text{-MAG} + AA \leftrightarrow 1,2\text{-DAG} + W \quad (18)$$

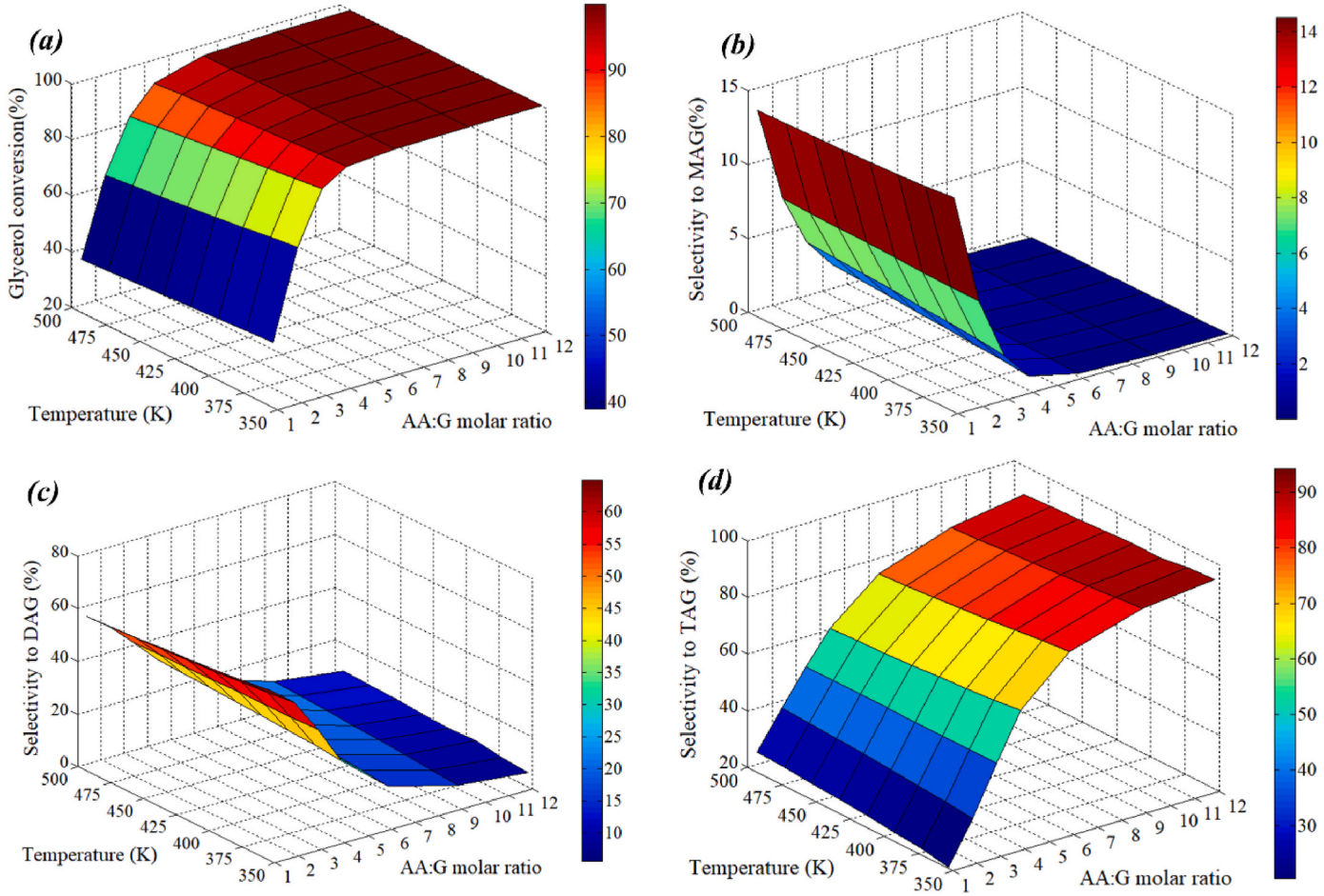

Fig. 3. Gibbs free energy minimization results as a function of temperature and the AA:G initial molar ratio: (a) Glycerol conversion; (b) Selectivity to MAG (1-MAG + 2-MAG); (c) Selectivity to DAG (1,2-DAG + 1,3-DAG); (d) Selectivity to TAG. P = 2 MPa.

2-MAG + AA ↔ 1,2-DAG + W (19)

1,3-DAG + AA ↔ TAG + W (20)

1,2-DAG + AA ↔ TAG + W (21)

Glycerol acetylation with acetic acid is an equilibrium reaction, so parameters such as temperature and reactants initial molar ratio can shift the equilibrium, favoring product formation. Fig. 3 shows the variation of glycerol conversion and selectivity to different products as a function of temperature and the AA:G initial molar ratio.

Regarding the thermal effect, the glycerol conversion decreases when the temperature is higher, revealing the global exothermicity of the system, as it has been reported by other authors in the literature [19,23,41–43].

As the reactions involved are reversible, it is expected that an increment in the AA concentration produces a shift of the equilibrium to the product formation, which would explain the increment of glycerol conversion when the AA:G molar ratio is higher, with the consecutive formation of 1,2-DAG and 1,3-DAG from 1-MAG and 2-MAG, and TAG from 1,2-DAG and 1,3-DAG. This effect has been reported by several authors by employing different catalysts, such as polydivinylbenzene-based solid acids [25], sulphuric acid-functionalized siliceous zirconia [44], heteropolyacids supported on polymeric material poly-vinylpyrrolidone [45], $Fe_3O_4/SiO_2–SO_4^{2-}$ [46] and $SbCl_5$ [47].

As it can be observed, the AA:G molar ratio affects glycerol conversion more sharply than the temperature, and the higher variation is observed at AA:G between 1 and 4. For example, at 353 K and 493 K, for a AA:G = 1, glycerol conversions of 43% and 39% are obtained, respectively, while for the same temperatures and AA:G = 4, glycerol conversions of 98.6% and 94% are obtained, respectively.

In this range of AA:G molar ratios, a 68% of maximum selectivity to TAG is obtained, which is the product that has received special interest because of its potential as oxygenate fuel additive for diesel or gasoline [11].

The results in Fig. 3 show that the glycerol conversion and selectivity to TAG increase when higher AA:G values are employed (Fig. 3a and d), jointly with a decrease in the selectivity to 1-MAG, 2-MAG, 1,2-DAG and 1,3-DAG (Fig. 3b and c). This is a consequence of the reaction system: as TAG is produced from 1,2-DAG and 1,3-DAG, which are also produced from 1-MAG and 2-MAG, an increase in TAG selectivity must produce a decrease in MAG's and DAG's selectivity. For this reason, AA:G molar ratios between 9 and 12 in the 350–500 K range should be employed to obtain total glycerol conversion (~100%) and high yields to TAG (>90%).

As water is a byproduct of the acetylation reaction, its presence in crude glycerol could affect the glycerol conversion and selectivity. About this, glycerol coming from the biodiesel synthesis is diluted in water, with a glycerol concentration of 60–80 wt%. Thus, the water effect over those parameters as a function of the temperature and AA:G molar ratio was studied, considering a water content of 40 wt% (Fig. 4). As it can be observed, as the water content increases, the glycerol conversion and the selectivity to TAG decrease. This effect is more remarkable for low AA:G molar ratios and high temperatures (Fig. 4b and d). For example, at 353 K and 0 wt% of water, equilibrium conversions for AA:G = 1, 2, 3, 6 are 44, 75, 93 and 99.8%, respectively, while with 40 wt% of water and the same values of AA: G, glycerol

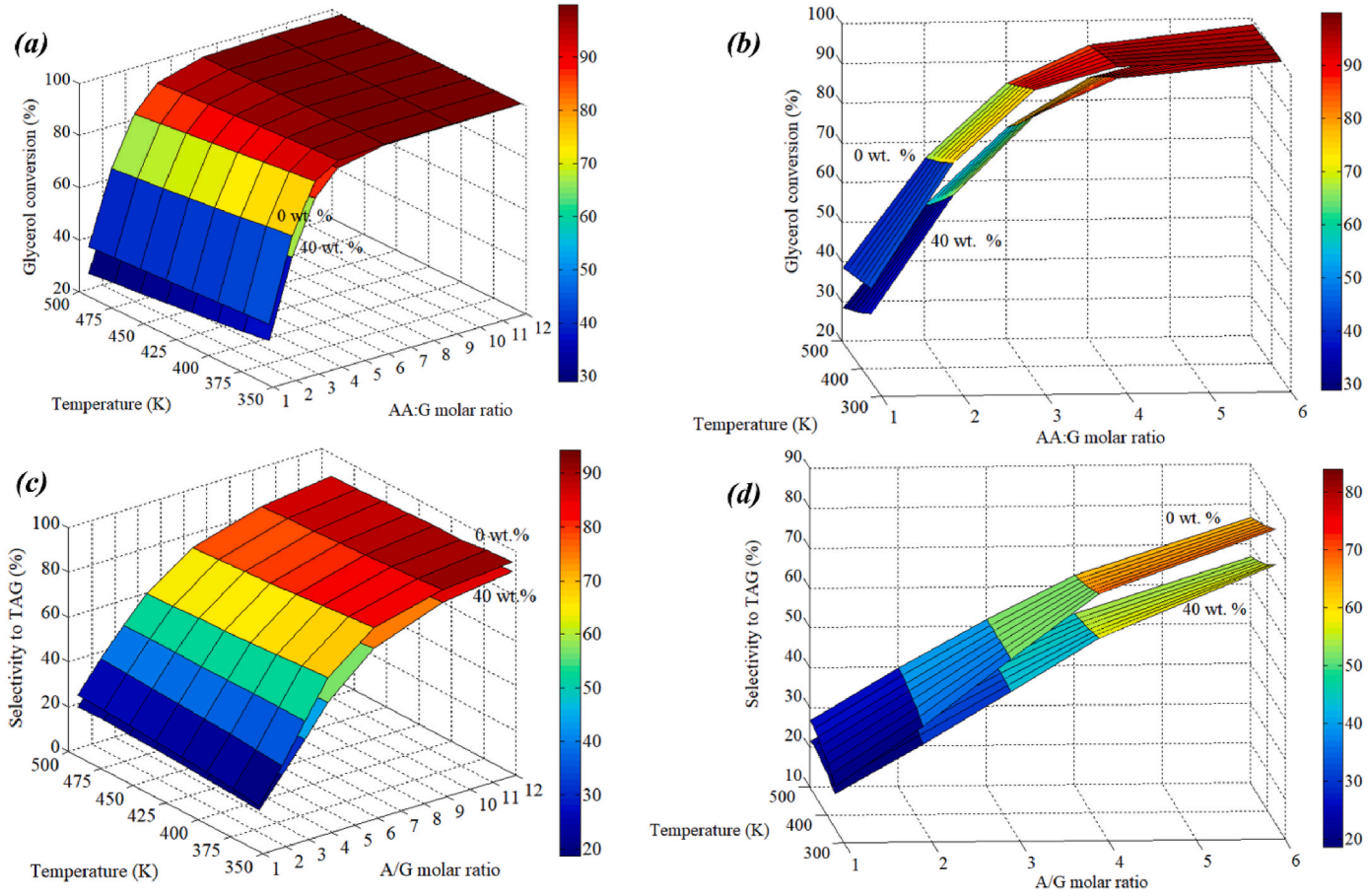

Fig. 4. Results of the Gibbs free energy minimization, considering the effect of the water initial content as a function of temperature and AA:G molar ratio. (a) Glycerol conversion; (b) Glycerol conversion: enlargement of the AA:G region between 1 and 6. (c) Selectivity to TAG and (d) Selectivity to TAG: enlargement of the AA:G region between 1 and 6. P = 2 MPa.

conversions are 37, 67, 87 and 99.4%, respectively. The figures of selectivity to MAG's and DAG's are shown in the Supplementary Information (Fig. S2).

As it can be observed, water produces a negative effect over the glycerol conversion and selectivity to TAG, so it is necessary to remove it from the reaction media in order to shift the equilibrium, favoring product formation. In this sense, Liu et al. synthesized a HZSM-5/MCM-41 catalyst and reached complete conversion of glycerol, with a selectivity to TAG of 91.3% at 125 °C and AA:G = 8, after 48 h of reaction. Our results show that selectivity to TAG would be 87.3% under the same conditions, but this difference could be due to the fact that water was continuously removed, shifting equilibrium to product formation [48]. On the other hand, Li et al. simulated a reactive distillation process for TAG production. Their results indicated that it is possible to obtain a complete glycerol conversion with high selectivity to TAG at the bottom of the column, using an AA:G molar ratio of 4, 50 theoretical stages for the reactive section, a reflux ratio between 4 and 6 and a top pressure of 35 kPa [43].

With the aim of verifying the results, the values obtained in this work were compared with those reported in the literature and experimentally obtained by other authors (Table 2).

As it can be observed, the solid catalysts presented in Table 2 achieved the glycerol conversion values predicted in this work. However, despite using an excess of AA, most of them cannot achieve the selectivity to TAG obtained in the present study. This phenomenon can be attributed to the nature of the serial mechanism (Eqs. (15)–(21)) in combination with the properties of the catalysts employed to perform the reactions. It is worth mentioning that the esterification reaction between glycerol and acetic acid occurs even without employing any catalyst, due to the autocatalytic effect caused by the acetic acid. In fact, Tonutti et al. reported that, after 5 h of reaction without catalyst at 393 K and an AA:G = 6, the glycerol conversion obtained is 100% with a selectivity to MAG and DAG of 45% and a selectivity to TAG of 10%. This information is essential to objectively compare the catalytic performance of different solids [40]. In this sense, the results in Table 2 indicate that almost all catalysts can achieve total glycerol conversion, as the first step in the reaction mechanism is not the limiting one in kinetic matter. However, most of them are limited to achieving high selectivity to TAG, indicating that the formation and consumption of 1, 2-DAG and 1,3-DAG are the slowest steps, as demonstrated by Tonutti et al. [40]. This could be attributed to the catalyst surface and their properties.

In this regard, Liu et al. demonstrated the importance of the acidity of the catalyst and the efficiency of diffusion of reactants and products in order to obtain high selectivity to TAG, because the size of this molecule (molecular diameter of ~4.5 nm) requires space to diffuse into the catalyst pores [48].

These requirements could explain some results shown in Table 2. For example, if the catalytic performance of the solid Sb_2O_5 (which presents a pore size of 18 nm and a Brønsted acid density of 0.035 mm g^{-1}) is compared with the blank test, it can be observed that the catalytic effect is almost negligible: 10% of glycerol conversion is achieved with the blank test, while 16.5% is obtained with this solid. This result can be attributed to the low acid density of the catalyst employed [53]. In addition, Ekinci and Oktar reported the hydrothermal synthesis of an MCM-41 catalyst, modified with silicotugnstic acid (STA) and zirconia (ZrO_2) (Table 2). The results showed a complete glycerol conversion, with a selectivity to TAG of 21%. Even though the presence of STA guarantees the existence of strong Brønsted acid sites, this solid presents a pore diameter of 1.9 nm, making more difficult the diffusion of reactants and products, fact that would explain the results obtained [54].

Considering these aspects, the efforts related to the synthesis of better catalysts should be focused on the obtention of higher selectivity to TAG, instead of improving the activity of the solid.

Fig. 5 represents the yield to TAG, calculated as the product between selectivity and glycerol conversion, for different catalytic systems as a function of the average pore diameter and the density of acid sites. The data was obtained from Table 2 considering only the catalysts whose textural and acidic properties were properly reported in the literature, as they seem to be critical in the formation of TAG.

As it can be seen from Fig. 5, the distribution of the dots indicates that, in order to obtain high yields to TAG, a catalyst should present suitable acid and textural properties. Materials such as phenolic resins (Amberlyst-15, Amberlyst-70), acidic mesoporous carbons (–SO_3H/

Table 2
Comparison of the results of this work with those reported in the literature. m_c: catalyst mass referred to glycerol (wt%). NI: Non-Informed.

Catalyst	AA: G	T (°C)	m_c (%)	t (h)	X_G (%)		S_{TAG} (%)		Ref.
					Exp.	Theor.	Exp.	Theor.	
PDSA-treated montmorillonite	3	120	NI	1	96	90.9	56.0	52.1	[49]
$SbCl_5$	4	80	5	0.25	100	95.7	22.0	57.2	[47]
$BuSnCl_3$	4	80	5	3.0	100	95.7	30.8	57.2	[50]
Y/SBA-3	4	110	4	2.5	100	93.7	55.0	56.1	[51]
Sulfonated carbonized rice husk	4	150	5	5.0	90	96.5	37.0	64.8	[52]
Blank Test	6	120	–	1.0	50	98.9	5.00	72.3	[40]
Blank Test	6	120	–	5.0	98	98.9	10.0	72.3	[40]
Amberlyst-70	6	105	5	10	100	99.8	87.6	82.9	[20]
Amberlyst-15	6	105	5	10	100	99.8	83.9	82.9	[20]
C-glycerol	6	110	9	2.0	97.0	99.0	23.0	73.0	[41]
Sb_2O_5	6	120	NI	3.5	96.3	98.9	12.6	72.3	[53]
Propyl–SO_3H–SBA-15	6	120	4	2.5	96	99.7	32.0	82.5	[22]
SO_4^{2-}/CeO_2–ZrO_2	6	120	5	1.0	100	98.9	16.5	72.3	[44]
STA-ZrO_2-MCM-41	6	200	4	4.0	100	96.9	21.0	68.1	[54]
Arenesulfonic acid functionalized bentonite	7	100	7	3.0	100	99.8	74.0	82.9	[55]
SSZ-550	9	80	3	0.7	100	99.9	93.0	85.7	[63]
SiO_2–H_3PO_4	9	100	5	4.0	100	99.9	22.8	84.6	[56]
Amberlyst-35	9	105	5	4.0	100	99.9	35.0	84.6	[5]
HZSM-5	9	110	11	4.5	85.6	99.8	7.70	84.0	[57]
HUSY	9	110	11	4.5	78.4	99.8	5.60	84.0	[57]
CsPWA	9	110	7	2.0	98.2	99.8	17.0	84.0	[42]
Sucrose-SBA-15-BDS	9	110	9	6.0	95	99.9	22.0	89.7	[58]
SO_4^{2-}/γ- Al_2O_3	9	110	5	5.0	97.0	99.8	23.1	84.0	[59]
Dowex 650C	9	120	4	6.0	99.6	99.8	37.0	83.5	[60]
–SO_3H/C–Si–Zr	9	150	9	5.0	97.0	99.9	93.8	88.7	[61]
20 mol% MnO_3/SiO_2	10	100	10	8.0	100	99.9	50.0	90.6	[62]
$H_4SiW_{12}O_{40}/ZrO_2$	10	120	6	4.0	100	99.9	32.3	89.7	[39]

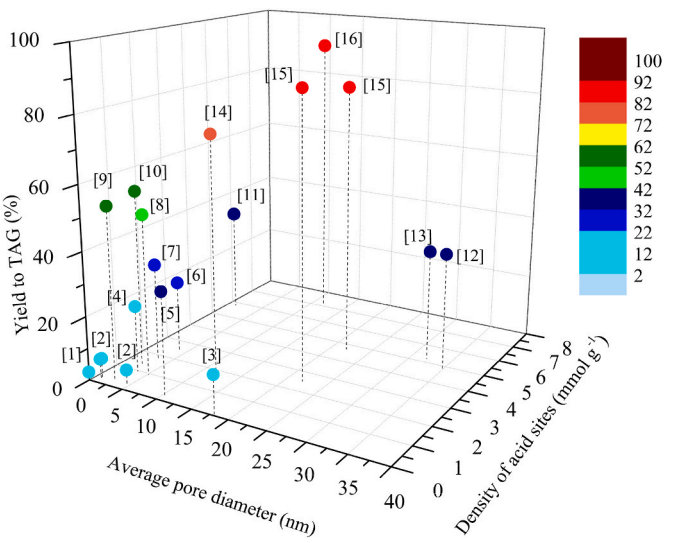

Fig. 5. Yield to TAG as a function of the average pore diameter and density of acid sites, extracted from reported data. [1]- [41]; [2]- [57]; [3]- [53]; [4]- [58]; [5]- [38]; [6]- [59]; [7]- [22]; [8]- [62]; [9]- [49]; [10]- [51]; [11]- [52]; [12]- [60]; [13]- [5]; [14]-[55]; [15]- [20]; [16]- [61].

C–Si–Zr) and sulphated siliceous zirconia catalysts (SSZ-550) combine a high density of acid sites with large average pore diameters, which allows obtaining high yields to TAG, similar to those predicted when the chemical equilibrium is reached [20,49,51,55,61].

As an example of this, yields to TAG of 88% and 84% can be obtained using Amberlyst-70 and Amberlyst-15, which are acidic ion-exchange resins with high density of Brønsted acid sites (2.55 and 4.70 $mmol g^{-1}$ respectively) and average pore diameters of 22 nm and 30 nm, respectively [20].

Other catalytic systems such as mesoporous carbon composites ($–SO_3H$/C–Si–Zr) with acid sites densities of 7 mmol g^{-1} and pore sizes of 10–20 nm, were suitable for obtaining TAG, achieving a selectivity of ~94% under the experimental conditions shown in Table 2. This value is slightly higher than the selectivity predicted in this work (88.7%), fact that could be explained considering the hydrophilicity of the solid [61]. Finally, Abida et al. synthesized a mesoporous sulphated siliceous zirconia catalyst (SSZ-550), which displayed high glycerol conversion levels and high selectivity to TAG (93%), due to the presence of strong Brønsted acidic sites (~5 mmol g^{-1}) in the form of sulphate groups ($SO_4–H^+$) [63].

4. Conclusions

In this work, the chemical equilibrium of the esterification reaction of glycerol (G) with acetic acid (AA) to form mono- (MAG), di- (DAG) and tri- (TAG) acetylglycerols was studied. Physicochemical and thermodynamic properties as a function of temperature (c_p^0, Δh_f^0, Δs_f^0 and Δg_f^0) of the compounds involved in the reaction were successfully calculated by implementing a group contribution method. The specific heat of glycerol at standard conditions (298 K and 101.325 kPa) presents a difference of 8% with respect to the reported value, and, for the rest of the compounds, this difference is between 1 and 3%, demonstrating the validity of the results obtained.

The minimization of the Gibbs free energy method was employed to obtain the compositions at the equilibrium, considering the non-ideality of the liquid phase by employing the UNIFAC method. The results showed that the glycerol conversion decreases when the temperature is higher, revealing the global exothermicity of the system. However, this variation is not too significant, attributed to the slightly variation of the specific heat of all compounds with temperature. Furthermore, the AA:G molar ratio affects glycerol conversion more sharply than temperature, showing the highest variation for AA:G molar ratios between 1 and 4. Nevertheless, the selectivity to TAG is lower under these conditions, so higher AA:G molar ratios should be employed in order to obtain a higher selectivity to the most substituted product.

The presence of water in the glycerol solution was also studied, indicating that it produces a decrease of the glycerol conversion and selectivity to TAG, which demands adequate strategies to remove water from the reaction medium.

With the aim of maximizing the selectivity to TAG, high molar ratios of AA:G should be used as well as catalytic systems with a combination of high density of acid sites and adequate pore size that ensure the accessibility of products and reagents to the active sites.

List of symbols

T^s	Standard temperature
P^s	Standard pressure
T	Temperature
P	Pressure
$\Delta h^s_{f,i}$	Molar enthalpy of formation of compound *i* at standard conditions
$\Delta s^s_{f,i}$	Molar entropy of formation of compound *i* at standard conditions
ν_j	Number of chemical groups of type *j* in the molecule *i*
$\Delta h^s_{f,j}$	Molar enthalpy of formation of the chemical group *j* at standard conditions
$\Delta s^s_{f,j}$	Molar entropy of formation of the chemical group *j* at standard conditions
$s^s_{f,j}$	Absolute molar entropy of chemical group *j*
s^s_m	Absolute molar entropy of element *m*
$c^0_{p,i}$	Specific heat of compound *i* at temperature T

Funding

This work was supported by the "Consejo Nacional de Investigaciones Científicas y Técnicas" (CONICET-PIP 0065), and the "Universidad Nacional de La Plata" (UNLP-I248).

Declaration of competing interest

The authors declare that they have no known competing financial interests or personal relationships that could have appeared to influence the work reported in this paper.

Acknowledgements

The doctoral fellowship granted by UNLP to Federico M. Perez is gratefully acknowledged.

$\Delta c^0_{p,i}$	Specific heat change of compound *i* with respect to the elements
$c^0_{p,m}$	Specific heat of the element *m*
α_m	Number of C atoms and H_2 and O_2 molecules present in compound *i*
$\Delta h^0_{f,i}$	Molar enthalpy of formation of compound *i* at temperature T
$\Delta s^0_{f,i}$	Molar entropy of formation of compound *i* at temperature T
$\Delta g^0_{f,i}$	Molar Gibbs free energy of formation of compound *i* at temperature T
n_i	Number of moles of compound *i* at equilibrium
k	Type of element (C, H, O)
K	Total number of elements in the system
A_k	Number of moles of element *k*
a_{ik}	Number of atoms of element *k* present in compound *i*
N	Number of compounds in the system
$\tilde{f}_i$	Partial fugacity of compound *i*
γ_i	Activity coefficient of compound *i*
x_i	Molar fraction of compound *i*
R	Gas constant
λ_k	Lagrange multiplier of element *k*
v_i^L	Specific volume of compound *i* in liquid phase
f_i^L	Fugacity of pure compound *i* in liquid phase
T_{ci}	Critical temperature of compound *i*
P_{ci}	Critical pressure of compound *i*
v_{ci}	Critical volume of compound *i*
ω_i	Acentric factor of compound *i*
X_G	Glycerol conversion
n_G^0	Initial number of moles of glycerol
n_G	Number of moles of glycerol at equilibrium
S_i	Selectivity to compound *i*
n_i	Number of moles of compound *i* at equilibrium
n_{H2O}	Number of moles of water at equilibrium
T_r	Reduced temperature

Appendix A. Supplementary data

Supplementary data to this article can be found online at https://doi.org/10.1016/j.rineng.2022.100502.

References

[1] A.O. Esan, A.D. Adeyemi, S. Ganesan, A review on the recent application of dimethyl carbonate in sustainable biodiesel production, J. Clean. Prod. 257 (2020), 120561, https://doi.org/10.1016/j.jclepro.2020.120561.

[2] I.N. Buffoni, M.N. Gatti, G.F. Santori, F. Pompeo, N.N. Nichio, Hydrogen from glycerol steam reforming with a platinum catalyst supported on a SiO2-C composite, Int. J. Hydrogen Energy 42 (2017) 12967–12977, https://doi.org/10.1016/j.ijhydene.2017.04.047.

[3] J. Kowalska-Kuś, A. Held, K. Nowińska, Solketal formation in a continuous flow process over hierarchical zeolites, ChemCatChem 12 (2020) 510–519, https://doi.org/10.1002/cctc.201901270.

[4] M.N. Gatti, J.L. Cerioni, F. Pompeo, G.F. Santori, N.N. Nichio, High yield to 1-propanol from crude glycerol using two reaction steps with Ni catalysts, Catalysts 10 (2020) 615, https://doi.org/10.3390/catal10060615.

[5] X. Liao, Y.Z. Sheng-Guang, W.Y. Li, Producing triacetylglycerol with glycerol by two steps: esterification and acetylation, Fuel Process. Technol. 90 (2009) 988–993, https://doi.org/10.1016/j.fuproc.2009.03.015.

[6] P.U. Okoye, A.Z. Abdullah, B.H. Hameed, A review on recent developments and progress in the kinetics and deactivation of catalytic acetylation of glycerol—a byproduct of biodiesel, Renew. Sustain. Energy Rev. 74 (2017) 387–401, https://doi.org/10.1016/j.rser.2017.02.017.

[7] X. Liao, Y. Zhu, S.G. Wang, H. Chen, Y. Li, Theoretical elucidation of acetylating glycerol with acetic acid and acetic anhydride, Appl. Catal., B 94 (2010) 64–70, https://doi.org/10.1016/j.apcatb.2009.10.021.

[8] N. Rahmat, A. Zuhairi, A. Abdul, R. Mohamed, Recent progress on innovative and potential technologies for glycerol transformation into fuel additives: a critical review, Renew. Sustain. Energy Rev. 14 (2010) 987–1000, https://doi.org/10.1016/j.rser.2009.11.010.

[9] A. Casas, J.R. Ruiz, M.J. Ramos, A. Pérez, Effects of triacetin on biodiesel quality, Energy Fuels 24 (2010) 4481–4489, https://doi.org/10.1021/ef100406b.

[10] U.I. Nda-Umar, I. Ramli, Y.H. Taufiq-Yap, E.N. Muhamad, An Overview of recent research in the conversion of glycerol into biofuels, fuel additives and other bio-based chemicals, Catalysts 9 (2018), https://doi.org/10.3390/catal9010015.

[11] Y. Sun, J. Hu, S. An, Q. Zhang, Y. Guo, D. Song, Q. Shang, Selective esterification of glycerol with acetic acid or lauric acid over rod-like carbon-based sulfonic acid functionalized ionic liquids, Fuel 207 (2017) 136–145, https://doi.org/10.1016/j.fuel.2017.06.073.

[12] C.E. Goncalves, L.O. Laier, M.J. da Silva, Novel esterification of glycerol catalysed by tin chloride (II): a recyclable and less corrosive process for production of bio-additives, Catal. Lett. 141 (2011) 1111–1117, https://doi.org/10.1007/s10562-011-0570-x.

[13] Y. Liu, E. Lotero, J.G. Goodwin Jr., Effect of water on sulfuric acid catalyzed esterification, J. Molec. Cat. A: Chem. 245 (2006) 132–140, https://doi.org/10.1016/j.molcata.2005.09.049.

[14] L.G. Wade, Whitman College, Organic Chemistry, eighth ed., Pearson, México, 2011.

[15] B. Meireles, V.L.P. Pereira, Synthesis of bio-additives: transesterification of ethyl acetate with glycerol using homogeneous or heterogeneous acid catalysts, J. Braz. Chem. Soc. 24 (2013) 17–25, https://doi.org/10.1590/S0103-50532013000100004.

[16] M.S. Khayoon, B.H. Hameed, Acetylation of glycerol to biofuel additives over sulfated activated carbon catalyst, Bioresour. Technol. 102 (2011) 9229–9235, https://doi.org/10.1016/j.biortech.2011.07.035.

[17] P.S. Kong, M.K. Aroua, W.M.A.W. Daud, H.V. Lee, P. Cognetc, Y. Peresc, Catalytic role of solid acid catalysts in glycerol acetylation for the production of bio-additives: a review, RSC Adv. 6 (2016), 68885, https://doi.org/10.1039/C6RA10686B.

[18] J. Lilja, D.Y. Murzin, T. Salmi, J. Aumo, P. Mäki-Arvela, M. Sundell, Esterification of different acids over heterogeneous and homogeneous catalysts and correlation with the Taft equation, J. Molec. Cat. A: Chem. 182–183 (2002) 555–563, https://doi.org/10.1016/S1381-1169(01)00495-2.

[19] Y. Jiang, X. Li, H. Zhao, Z. Hou, Esterification of glycerol with acetic acid over SO3H-functionalized phenolic resin, Fuel 255 (2019), 115842, https://doi.org/10.1016/j.fuel.2019.115842.

[20] S. Kale, S.B. Umbarkar, M.K. Dongare, R. Eckelt, U. Armbruster, A. Martin, Selective formation of triacetin by glycerol acetylation using acidic ion-exchange resins as catalyst and toluene as an entrainer, Appl. Catal. A 490 (2015) 10–16, https://doi.org/10.1016/j.apcata.2014.10.059.

[21] A. Patel, S. Singh, A green and sustainable approach for esterification of glycerol using 12-tungstophosphoric acid anchored to different supports: kinetics and effect of support, Fuel 118 (2014) 358–364, https://doi.org/10.1016/j.fuel.2013.11.005.

[22] B.O. Dalla Costa, H.P. Decolatti, M.S. Legnoverde, C.A. Querini, Influence of acidic properties of different solid acid catalysts for glycerol acetylation, Catal. Today 289 (2017) 222–230, https://doi.org/10.1016/j.cattod.2016.09.015.
[23] P. Arun, S.M. Pudi, P. Biswas, Acetylation of glycerol over sulfated alumina: reaction parameter study and optimization using response surface methodology, Energy Fuels 20 (2016) 584, https://doi.org/10.1021/acs.energyfuels.5b01901.
[24] A. Neto, A. Oliveira, E. Rodriguez-Castellón, A. Campos, P. Freire, F. Sousa, J. Filho, J. Araujo, R. Lang, A comparative study on porous solid acid oxides as catalysts in the esterification of glycerol with acetic acid, Catal. Today 349 (2020) 57–67, https://doi.org/10.1016/j.cattod.2018.05.057.
[25] R. Mou, X. Wang, Z. Wang, D. Zhang, Z. Yin, Y. Lv, Z. Wei, Synthesis of fuel bioadditive by esterification of glycerol with acetic acid over hydrophobic polymer-based solid acid, Fuel 302 (2021), 121175, https://doi.org/10.1016/j.fuel.2021.121175.
[26] W.R. Smith, R.W. Missen, Chemical Reaction Equilibrium Analysis: Theory and Algorithms, Wiley, 1982.
[27] E. Domalski, E. Hearing, Estimation of the thermodynamic properties of C-H-N-O-S-halogen compounds at 298.15 K, J. Phys. Chem. Ref. Data 22 (1993) 805–1159, https://doi.org/10.1063/1.555927.
[28] V. Růžička, E. Domalski, Estimation of the heat capacities of organic liquids as a function of temperature using group Additivity. I. Hydrocarbon compounds, J. Phys. Chem. Ref. Data 22 (1993) 597–618, https://doi.org/10.1063/1.555923.
[29] B. Poling, J. Prausnitz, J. O'Connell, The Properties of Gases and Liquids, fifth ed., McGraw Hill, New York, 2001.
[30] NIST database. https://webbook.nist.gov/. (Accessed March 2022).
[31] T. Yamada, R.D. Gunn, Saturated liquid molar volumes. Rackett equation, J. Chem. Eng. Data 18 (1973) 234–236, https://doi.org/10.1021/je60057a006.
[32] K.G. Joback, R.C. Reid, Estimation of pure-component properties from group-contributions, Chem. Eng. Commun. 157 (1987) 233–243, https://doi.org/10.1080/00986448708960487.
[33] Y. Nannoolal, J. Rarey, D. Ramjugernath, W. Cordes, Estimation of pure component properties: Part 1. Estimation of the normal boiling point of non-electrolyte organic compounds via group contributions and group interactions, Fluid Phase Equil. 226 (2004) 45–63, https://doi.org/10.1016/j.fluid.2004.09.001.
[34] D. Ambrose, J. Walton, Vapour pressures up to their critical temperatures of normal alkanes and 1-alkanols, Pure Appl. Chem. 61 (1989) 1395–1403, https://doi.org/10.1351/pac198961081395.
[35] A.K. Coker, Fortran Programs for Chemical Process Design, Analysis, and Simulation, first ed., Gulf Professional Publishing, 1995.
[36] J.C. Phillips, M.M. Mattamal, Correlation of liquid heat-capacities for carboxylic esters, J. Chem. Eng. Data 21 (1976) 228–232, https://doi.org/10.1021/je60069a030.
[37] X. Zhu, D.M. Phinney, S. Paluri, D.R. Heldman, Prediction of liquid specific heat capacity of food lipids, J. Food Sci. 83 (2018) 992–997, https://doi.org/10.1111/1750-3841.14089.
[38] S. Zhu, X. Gao, F. Dong, Y. Zhu, H. Zheng, Y. Li, Design of a highly active silver-exchanged phosphotungstic acid catalyst for glycerol esterification with acetic acid, J. Catal. 306 (2013) 155–163, https://doi.org/10.1016/j.jcat.2013.06.026.
[39] S. Zhu, Y. Zhu, X. Gao, T. Mo, Y. Zhu, Y. Li, Production of bioadditives from glycerol esterification over zirconia supported heteropolyacids, Bioresour. Technol. 130 (2013) 45–51, https://doi.org/10.1016/j.biortech.2012.12.011.
[40] L.G. Tonutti, B.O. Dalla Costa, H.P. Decolatti, G. Mendow, C.A. Querini, Determination of kinetic constants for glycerol acetylation by particle swarm optimization algorithm, Chem. Eng. J. 424 (2021), 130408, https://doi.org/10.1016/j.cej.2021.130408.
[41] J.A. Melero, R. van Grieken, G. Morales, M. Paniagua, Acidic mesoporous silica for the acetylation of glycerol: synthesis of bioadditives to petrol fuel, Energy Fuels 21 (2007) 1782–1791, https://doi.org/10.1021/ef060647q.
[42] G.A. Bedogni, C.L. Padró, N.B. Okulik, A combined experimental and computational study of the esterification reaction of glycerol with acetic acid, J. Mol. Model. 20 (2014) 2167, https://doi.org/10.1007/s00894-014-2167-y.
[43] H. Li, J. Li, X. Li, X. Gao, Esterification of glycerol and acetic acid in a pilot-scale reactive distillation column: experimental investigation, model validation, and process analysis, J. Taiwan Inst. Chem. Eng. 89 (2018) 56–66, https://doi.org/10.1016/j.jtice.2018.05.009.
[44] P.S. Reddy, P. Sudarsanam, G. Raju, B.M. Reddy, Selective acetylation of glycerol over CeO2-M and SO42-/CeO2-M (M = ZrO2 and Al2O3) catalysts for synthesis of bio additives, J. Ind. Eng. Chem. 18 (2012) 648–654, https://doi.org/10.1016/j.jiec.2011.11.063.
[45] S. Magar, G.T. Mohanraj, S.K. Jana, C.V. Rode, Synthesis and characterization of supported heteropoly acid: efficient solid acid catalyst for glycerol esterification to produce biofuel additives, Inorg. Nano-Metal Chem. 50 (2020) 1157–1165, https://doi.org/10.1080/24701556.2020.1737817.
[46] K. Abida, B. Chudasama, A. Ali, Development and functionalization of magnetic nanoparticles as stable and reusable catalysts for triacetin synthesis, New J. Chem. 44 (2020) 9365–9376, https://doi.org/10.1039/D0NJ00488J.
[47] F.M.R.S. Altino, D.S. da Silva, J.H. Bortoluzzi, S.M.P. Meneghetti, Investigation of Glycerol Acetylation in the Presence of Sb Catalysts, Biomass Convers. and Biorefinery, 2021, https://doi.org/10.1007/s13399-021-01318-y.
[48] J. Liu, Z. Wang, Y. Sun, R. Jian, P. Jian, D. Wang, Selective synthesis of triacetin from glycerol catalyzed by HZSM-5/MCM-41 micro/mesoporous molecular sieve, Chin. J. Chem. Eng. 27 (2019) 1073–1078, https://doi.org/10.1016/j.cjche.2018.09.013.
[49] N.J. Venkatesha, Y.S. Bhat, B.S.J. Prakash, Volume accessibility of acid sites in modified montmorillonite and triacetin selectivity in acetylation of glycerol, RSC Adv. 6 (2016) 45819–45828, https://doi.org/10.1039/C6RA05720A.
[50] D.S. da Silva, F.M.R.S. Altino, J.H. Bortoluzzi, S.M.P. Meneghetti, Investigation of Sn (IV) catalysts in glycerol acetylation, Mol. Catal. 494 (2020), 111130, https://doi.org/10.1016/j.mcat.2020.111130.
[51] M.S. Khayoon, S. Triwahyono, B.H. Hameed, A.A. Jalil, Improved production of fuel oxygenates via glycerol acetylation with acetic acid, Chem. Eng. J. 243 (2014) 473–484, https://doi.org/10.1016/j.cej.2014.01.027.
[52] T.S. Galhardo, N. Simone, M. Goncalves, F.C.A. Figueiredo, D. Mandelli, W. A. Carvalho, Preparation of sulfonated carbons from rice husk and their application in catalytic conversion of glycerol, ACS Sustainable Chem. Eng. 1 (2013) 1381–1389, https://doi.org/10.1021/sc400117t.
[53] W. Hu, Y. Zhang, Y. Huang, J. Wang, J. Gao, J. Xu, Selective esterification of glycerol with acetic acid to diacetin using antimony pentoxide as reusable catalyst, J. En. Chem. 24 (2015) 632–636, https://doi.org/10.1016/j.jechem.2015.08.001.
[54] E.K. Ekinci, N. Oktar, Production of value-added chemicals from esterification of waste glycerol over MCM-41 supported catalysts, Green Process. Synth. 8 (2019) 128–134, https://doi.org/10.1515/gps-2018-0034.
[55] M. Tangestanifard, H.S. Ghaziaskar, Arenesulfonic acid-functionalized bentonite as catalyst in glycerol esterification with acetic acid, Catalysts 7 (2017) 211, https://doi.org/10.3390/catal7070211.
[56] R. Manurung, M.D. Anggreawan, A.G. Siregar, Triacetin production using SiO2-H3PO4 catalysts derived from bamboo leaf biomass waste for esterification reactions of glycerol and acetic acid, IOP Conf. Ser. Mater. Sci. Eng. 801 (2020), 012052, https://doi.org/10.1088/1757-899X/801/1/012052.
[57] L. Zhou, E. Al-Zaini, A.A. Adesina, Catalytic characteristics and parameters optimization of the glycerol acetylation over solid acid catalysts, Fuel 103 (2013) 617–625, https://doi.org/10.1016/j.fuel.2012.05.042.
[58] J. Goscianska, A. Malaika, A facile post-synthetic modification of ordered mesoporous carbon to get efficient catalysts for the formation of acetins, Catal. Today 357 (2020) 84–93, https://doi.org/10.1016/j.cattod.2019.02.049.
[59] S.A. Rane, S.M. Pudi, P. Biswas, Esterification of glycerol with acetic acid over active and stable Alumina-based catalysts: a reaction kinetics study, Chem. Biochem. Eng. Q. 30 (2016) 33–45, https://doi.org/10.15255/CABEQ.2014.2093.
[60] D.M. Reinoso, D.E. Boldrini, Kinetic study of fuel bio-additive synthesis from glycerol esterification with acetic acid over acid polymeric resin as catalyst, Fuel 264 (2020), 116879, https://doi.org/10.1016/j.fuel.2019.116879.
[61] S. Kumar, N. Viswanadham, S.K. Saxena, A. Selvamani, J. Diwakar, A.H. Al-Muhtaseb, Single-pot template-free synthesis of a glycerol-derived C–Si–Zr mesoporous composite catalyst for fuel additive production, New J. Chem. 44 (2020) 8254–8263, https://doi.org/10.1039/D0NJ00523A.
[62] T.V. Kotbagi, S.L. Pandhare, M.K. Dongare, S.B. Umbarkar, In situ formed supported silicomolybdic heteropolyanions: efficient solid catalyst for acetylation of glycerol, J. Environ. Anal. Chem. 2 (2015), https://doi.org/10.4172/2380-2391.1000160.
[63] K. Abida, A. Ali, Sulphuric acid-functionalized siliceous zirconia as an efficient and reusable catalyst for the synthesis of glycerol triacetate, Chem. Pap. 74 (2020) 3627–3639, https://doi.org/10.1007/s11696-020-01189-z.
[64] A. Fredenslund, R.L. Jones, J.M. Prausnitz, Group-contribution estimation of activity coefficients in nonideal liquid mixtures, AlChE J. 21 (1975) 1086–1099, https://doi.org/10.1002/aic.690210607.
[65] D. Green, R. Perry, Perry's Chemical Engineers' Handbook, Eight edition, McGraw Hill, New York, 2008.